## Title

Reliability of low frequency mHVSR ordinates



## Authors

Ornelas, Francesco Javier
Nweke, CC
de la Torre, Christopher A
et al.

## Publication Date

2024-07-01

Peer reviewed

18TH WORLD CONFERENCE ON EARTHQUAKE ENGINEERING
WCEE2024
MILAN

MILAN, ITALY
30TH JUNE - 5TH JULY 2024

www.wcee2024.it

# RELIABILITY OF LOW FREQUENCY MHVSR ORDINATES

F.J. Ornelas[1], C.C. Nweke[2], C.A. de la Torre[3], P. Wang[4], T.D. Mai[5], B.R. Cox[6], S.J. Brandenberg[7], and J.P. Stewart[8]

[1] Graduate Student Researcher, University of California, Los Angeles, USA, jornela1@g.ucla.edu
[2] Assistant Professor, University of Southern California, Los Angeles, USA
[3] Post-Doctoral Fellow, University of Canterbury Christchurch, NZ
[4] Assistant Professor, Old Dominion University Norfolk, USA
[5] Graduate Student, University of Southern California, Los Angeles, USA
[6] Professor, Utah State University, Logan, USA
[7] Professor, University of California, Los Angeles, USA
[8] Professor, University of California, Los Angeles, USA

**Abstract**: *Microtremor horizontal-to-vertical spectral ratios (mHVSR) are frequency-dependent ratios of Fourier amplitude spectra of the horizontal to vertical components of a 3-component recording of ambient ground motions from microtremors. Results from mHVSR tests can identify the frequencies associated with site resonances at sites with large impedance contrasts, and hence have potential to provide useful parameters for predicting seismic site response. Site measurements are made by recording ground vibrations either from a temporarily deployed seismometer, typically recording for a relatively short period of time (~1-2 hrs.), or from a permanently-installed broadband seismometer. In this paper, we discuss ongoing work investigating the reliability of low frequency (< ~0.1 Hz) mHVSR ordinates. Such low frequency ordinates are potentially useful for sites that are known to have deep basins (e.g., LA Basin, Imperial Valley, Great Salt Lake basin), where fundamental frequencies may fall in this range and direct measurements of depth to bedrock are difficult to make. We have found that low-frequency mHVSR ordinates (< ~0.1-0.2 Hz) are for practical purposes not reliable in most cases, even when measured by high-quality temporary or permanent broadband sensors. In this paper, we discuss sensor drift and its limited impact on the reliability of mHVSR ordinates. We document the low frequency problem for multiple sites, although we do not have a solution as of this writing for how to improve the reliability of low-frequency results.*

## 1. Introduction

Microtremor horizontal-to-vertical spectral ratios (mHVSR) can be used to identify resonant frequencies using a 3-component seismometer measuring ambient vibrations or microtremors. The sources of these ambient vibrations are typically natural (wind, ocean waves, etc.) and anthropogenic (i.e., traffic, machinery, etc.). Wilson et al. (2002) evaluated sources of seismic signals across different frequency bands, finding that low frequencies (< 0.1 Hz) are dominated by thermal or atmosphere-driven local slab-tilt effects, mid-frequencies (0.1-0.3 Hz) are dominated by naturally occurring microseismic noise, and high-frequency (0.3-8 Hz) ambient vibrations are derived primarily from cultural sources.

Nakamura (1989) found that by assuming that the horizontal components of a shear wavefield are amplified whereas the vertical components are not, for sites with large impedance contrasts, resonant frequencies of the site can be evaluated from peaks in mHVSR spectrum. Subsequent research found that the lowest peak in an mHVSR spectrum identifies the fundamental frequency, $f_0$ (Lermo and Chavez-Garcia 1993; Lachet et. al. 1996; Theodulidis et. al. 1996; Bonilla et. al. 2002; Kawase et. al. 2011; Cadet et. al. 2012; Ghofrani et. al. 2013). However, many of these early studies only identified peaks at frequencies greater than 0.1 Hz. Given

the different noise sources at low frequencies (Wilson et al. 2002, Given and Fels 1993), it remains an open question whether lower frequency peaks have a clear relationship to site resonances.

In this paper, we share our findings from a series of recent site measurements in which the reliability of mHVSR ordinates at low frequencies appears to be questionable. We discuss the processing procedures applied to the data, the sensitivity of mHVSR to those procedures, the effects of different sensor deployment depths in the field on mHVSR, and mHVSR differences between co-located temporary and permanently-installed instruments.

## 2. mHVSR Data Collection

### 2.1. Temporary Stations

mHVSR data were collected for 16 sites across California, each having a vertical (downhole) array (Ornelas et. al. 2023) in which the permanent seismic instruments are accelerometers. The 16 sites were previously investigated for site response modelling purposes by Afshari et al. (2019) and de la Torre et. al. (2022). Table 1 shows the names and locations of these sites. It has previously been shown that accelerometers do not produce reliable mHVSR results (Wang et. al. 2023), so data were collected using temporarily-deployed broadband seismometers at these 16 sites. These mHVSR surveys were performed using Nanometrics trillium compact horizon broadband (BB) seismometers with Pegasus PGS-140 digitizers. The sensors had a corner frequency of 120 sec. and the usable frequency range from sensor documentation is 0.0083 Hz to 100 Hz. The tests were performed in concentric circles, each expanding further from the vertical array, with four tests performed along each circle where possible. Tests were performed for about 1-2 hours at different times of the day deploying about 5 sensors at a time. The target radial distance from the vertical array for each circle was 50, 100, 250, and 500 m. Figure 1 shows an example of the proposed test layout, which in some cases was not achievable due to site restrictions. The sensors were buried such that the bottom of the sensor was 2-4 inches below the surface, when possible, to provide good coupling and to avoid excess drift from occurring and distorting the spectra at lower frequencies. Moreover, we also utilized a plastic 19-liter bucket to cover the sensor and prevent excess wind noise from affecting the recordings.

*Table 1: Description of each vertical array site where mHVSR surveys were performed. Stations based on vertical array sites that were analysed in Afshari et. al. (2019)*

| Station No. | CSMIP Station No. | Station Name | Latitude | Longitude |
|---|---|---|---|---|
| 2 | 68323 | Benicia-Martinez South | 38.03351 | -122.117 |
| 3 | 68206 | Crockett-Martinez | 38.05394 | -122.225 |
| 4 | 1794 | El Centro-Meloland | 32.77393 | -115.449 |
| 7 | UCSB Arrays | Hollister | 36.75758 | -121.613 |
| 8 | 58798 | Hayward-San Mateo | 37.61694 | -122.154 |
| 9 | 24703 | La Cienega | 34.03621 | -118.378 |
| 10 | 24400 | Obregon Park | 34.03701 | -118.178 |
| 11 | 23792 | San Bernardino | 34.06369 | -117.298 |
| 12 | 68310 | Vallejo-Hwy 37 | 38.1217 | -122.275 |
| 14 | 67266 | Antioch-San Joaquin S. | 38.01792 | -121.751 |
| 15 | 13186 | Corona | 33.88171 | -117.549 |
| 16 | 3192 | Coronado East | 32.69825 | -117.145 |
| 17 | 3193 | Coronado West | 32.68815 | -117.164 |
| 18 | 58798 | Foster City-San Mateo | 37.57276 | -122.264 |
| 19 | 58487 | Hayward-580W | 37.68868 | -122.107 |
| 20 | 58961 | San Francisco Bay Bridge | 37.7866 | -122.389 |

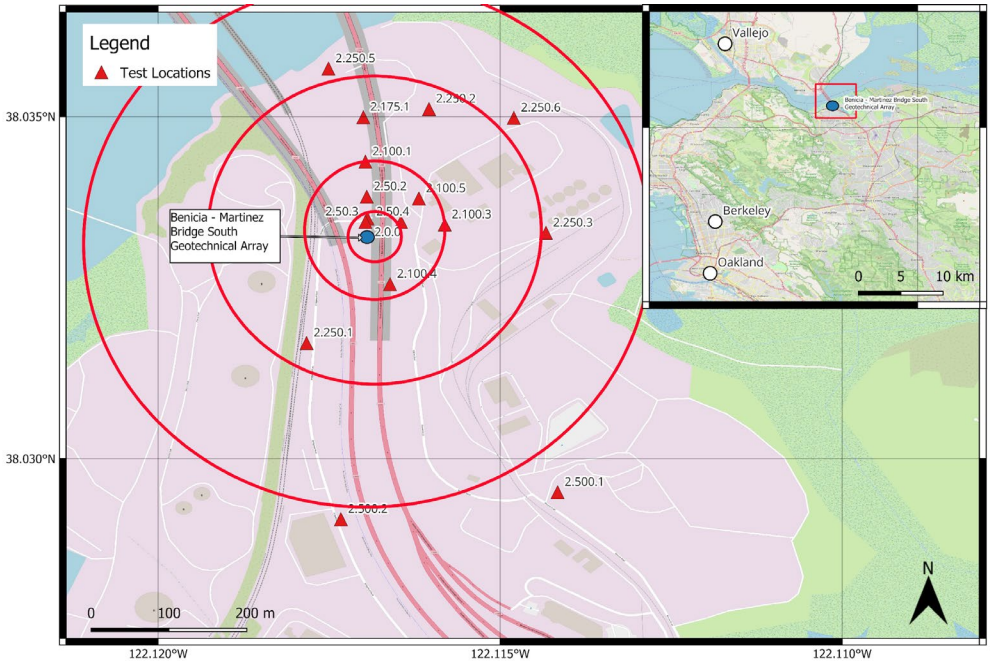


*Figure 1. Image of approximate layout followed when conducting mHVSR surveys. This image was for station 2 used for this study (see table 1) which is the Benicia-Martinez vertical array.*

### 2.2. Permanent Stations

Permanent stations were also used for the study to facilitate comparisons between mHVSR curves derived from temporary and permanent deployments. We collected data from the Incorporated Research Institution for Seismology (IRIS) and the Southern California Earthquake Data Center (SCEDC) (IRIS DMC 2020, SCEDC 2013). We specifically looked at sites where we had deployed temporary BB seismometers, and a permanent seismometer was nearby. In this paper, we will discuss findings from a site in Cabazon, CA (Section 4.1).

## 3. mHVSR Data Processing

### 3.1. Drift and Wobble

mHVSR ordinates are computed by taking the ratio between the horizontal and vertical components of a Fourier Amplitude Spectra (FAS). The processing procedures that were used to compute mHVSR, are described in Wang et. al. (2023), which is a modification of SESAME (2004) and Wathelet (2020). When we initially processed the data from the sites in Table 1, there were many cases where the data had appreciable sensor drift across the duration of the records, particularly in the vertical component. In Figure 2, this drift is observed in the vertical component as an approximately exponential decay. Moreover, large amplitude, long period oscillations (referred to subsequently as “wobble”) are apparent in the horizontal components (the period of these oscillations is approximately 200 s). This drift at the site in Figure 1 (station: 2.250.2), and other sites with similar results, motivated us to investigate methods for processing microtremor data so as to enhance the reliability of low-frequency mHVSR ordinates.

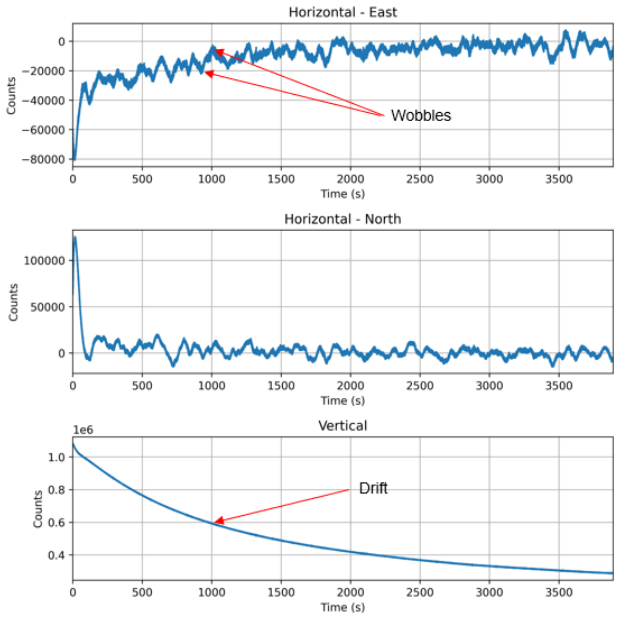


Figure 2. Raw time series for all three components of Benicia-Martinez South downhole vertical array, Station: 2.250.2, showing the drift that is occurring in all components, but specifically the vertical.

### 3.2 Windowing and Spectral Leakage

The data used in this study was typically recorded for about 1-2 hours. The initial procedure that was used to process the data was to break down a 60-min (3600 sec.) record into individual windows of 300 seconds. This allowed us to have 12 windows to average-across when computing the mean mHVSR curve. Allowing for at least 10 cycles per window, the theoretical lowest usable frequency was then 10/300 = 0.03 Hz. It is important to have at least 10 cycles per window to reliably capture mHVSR ordinates as recommended by SESAME (2004).

Figure 3 shows normalized time series which have been separated into discrete 300-second-long-time windows (indicated by alternating colors of blue and pink) where a Tukey (Tukey 1967) windowing function (sometimes referred to as a Cosine-Taper windowing function) and high-pass filter (Butterworth 1930) of 0.01 Hz are applied to each window. The processing was performed using the code *hvsrProc* by Wang (2021). The as-recorded motions in these plots have not been pre-processed (described in Section 3.3) to remove the drift. The large spikes at the edges of windows for the vertical component are a consequence of drift not having been removed prior to windowing. Much of the vertical component data that was processed generated features similar to those seen in Figure 3. Moreover, we observe that long period wobble in the horizontal components from Figure 2 causes issues within the 300-second-long-time windows, where gaps form within the windows.

These issues affect Fourier amplitudes of this data across a wide frequency range as a result of spectral leakage, potentially distorting mHVSR ordinates. Spectral leakage can be caused by taking the FFT of a window that is not stationary, which could affect all of the components in Figure 3 but would be strongest for the vertical component due to the pronounced drift. The distortion of the Fourier amplitudes from spectral leakage can make the vertical components larger than the horizontal components at low frequencies, thus lowering mHVSR ordinates. Because this is not a true representation of the ground conditions, we updated our procedures to correct for signal drift prior to computing mHVSR ordinates (section 3.3).

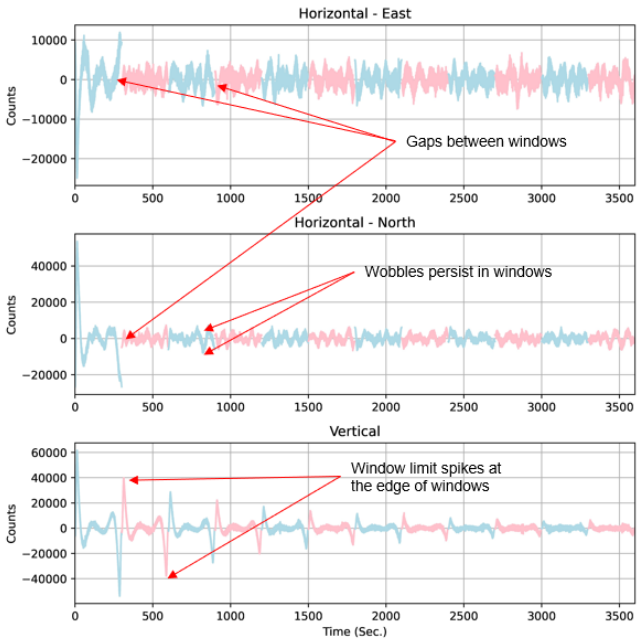


*Figure 3. Normalized time series from hvsrProc for data shown in Figure 2 showing discrete 300-second-long-time windows. These windows have been filtered by 0.01 Hz, Tukey windowed by 5 percent taper, and demeaned, which does not correct the drift in the vertical component. The components are East(top), North(middle), Vertical(bottom).*

### 3.3 Pre-Processing Procedures to Remove Spectral Leakage

We sought to develop new procedures to stabilize the time series data prior to processing the mHVSR data. Recording data after long "settling" periods (time when the sensor is equilibrating or stabilizing its internal reference due to configuration or deployment setup) could reduce but would not likely eliminate drift. As a practical matter, we aim to have procedures that would be effective for short-duration (60 min) deployments. Drift removal was applied with the following steps:

1. Demeaning of the entire time history: This entails subtracting a weighted mean, where the weight is taken from a Tukey window (Tukey 1967) applied to the entire time series.
2. Apply a Cosine-tapered window or a Tukey window to the entire time history after de-meaning
3. Filter the entire time history: This entails applying a high-pass Butterworth filter (Butterworth 1930). We have found that the mHVSR results are relatively insensitive to the corner frequency ($f_{cHP}$) within reasonable bounds, and for the plots herein we have used $f_{cHP}$ = 0.042 Hz. The corner frequency for a Butterworth filter is at the point at which the amplitude is 0.7. Ordinates are not appreciably affected by the filter for frequencies $f > 1.25f_{cHP}$. Accordingly, $1.25f_{cHP}$ = 0.042 Hz comprises the lowest usable frequency.

After applying these steps, the signal is stationary, as shown in Figure 4 for the Benicia-Martinez station site: 2.250.2. We would anticipate that the stabilized signal would produce more reliable mHVSR spectral ordinates. Figure 5 shows mHVSR curves for sites 2 and 9 from Table 1 (Benicia-Martinez and La Cienega) derived from the data with and without drift removal. Without pre-processing (blue line), the mHVSR ordinates appear to be stable at low frequencies, but they only appear this way because the vertical component is contaminated by spectral leakage, which is causing the vertical component to be nearly the same amplitude as the horizontal components. Following pre-processing, the stationary signals produce the mHVSR shown in orange lines in Figure 5.

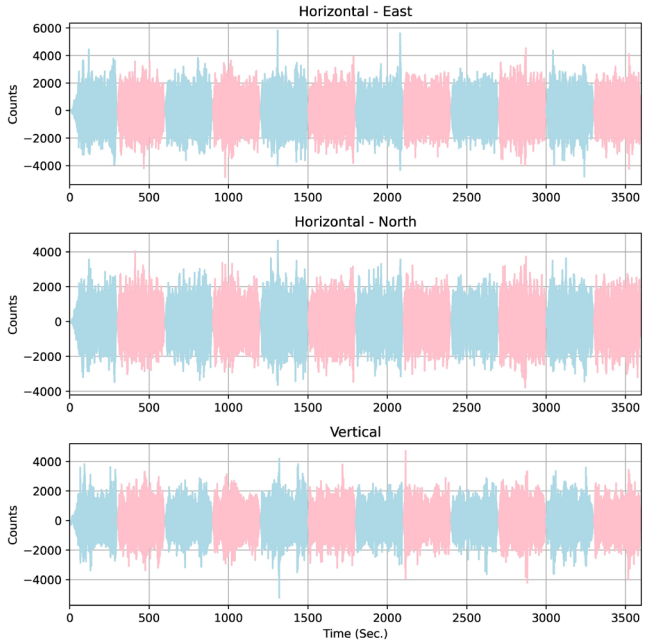


*Figure 4. Normalized time series from hvsrProc from data shown in Figure 2, showing discrete 300-second-long-time windows. The windows have been filtered by 0.01 Hz, Tukey windowed by 5 percent taper, and demeaned, which have corrected the drift and wobble in all components. The components are East(top), North(middle), Vertical(bottom).*

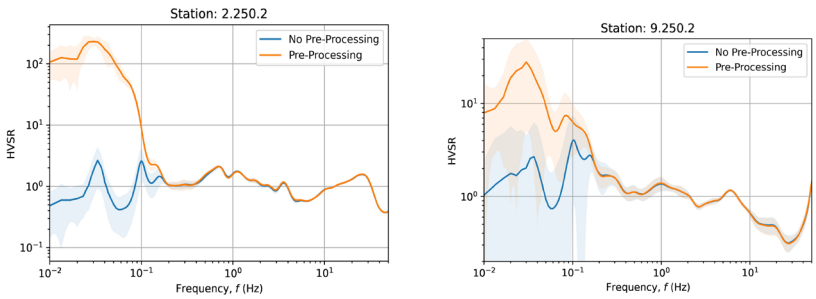


*Figure 5. (a) left: mHVSR mean curves with standard deviations for site 2.250.2 in Benicia-Martinez South downhole vertical array. (b) right: mHVSR mean curves with standard deviations for site 9.250.2 in La Cienega downhole vertical array. This shows how implementing different processing procedures can have drastic effects on low frequency mHVSR. Also, regardless of location, the same peak characteristics are present at frequencies below 0.1 Hz.*

As shown by the orange curves in Figure 5, at frequencies <~0.2 Hz, mHVSR ordinates increase markedly (by about one to two orders of magnitude). The resulting mHVSR curves for both sites have a peak at approximately 0.03 Hz, which is close to the $f_{cHP}$. Figure 6 shows that similar features are observed at additional sites discussed in Section 2.1. As shown in Figure 7, these peaks are caused by a sudden change in Fourier amplitudes in the vertical component due to the application of these processing steps discussed above. We are investigating the causes of the peaks, which may be due to the high-pass filter or tapering (this subject remains under investigation). Either way, the peak in the orange curves in Figure 5 near 0.03 Hz has no site-related physical meaning. Moreover, the low-frequency ordinates themselves, even at frequencies above the peak (0.03-0.1 Hz), seem to have no clear relationship to site properties. At higher frequencies (>0.1 Hz) the signal remains unaffected whether the pre-processing steps are applied or not.

We were initially surprised at these findings, given that the sensors used in the deployments are expected to be usable to much lower frequencies (~0.0083 Hz) than those where problems emerge. This is concerning, because we are interested in using mHVSR to evaluate resonances in deep basins (e.g., LA, Ventura, Imperial Valley basins), which would appear to be impossible based on these results. Some additional investigations related to this subject have been undertaken to further investigate the issue, as described subsequently.

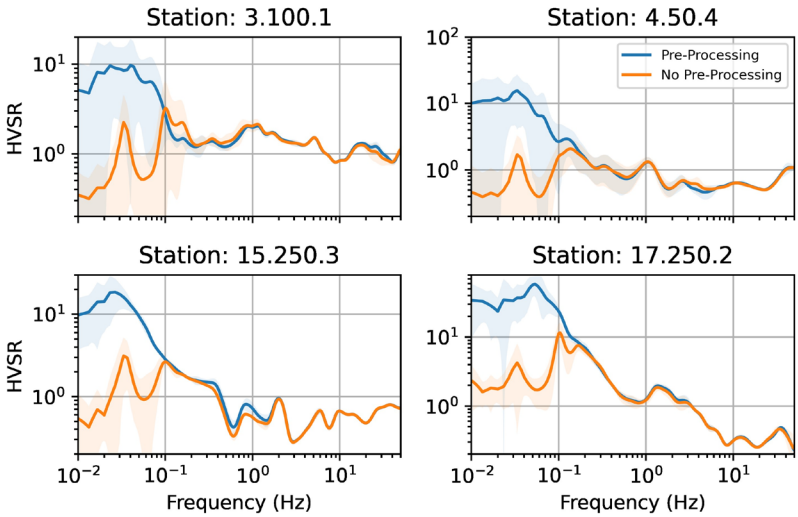


*Figure 6. mHVSR spectra for 4 different sites, (a) top left: Station 3.100.1 Crockett-Martinez, (b) top right: Station 4.50.4 El Centro-Meloland, (c) bottom left: Station 15.250.3 Corona, (d) bottom right: Station 17.250.2 Coronado West, each site showing the same peak feature at the same frequency of around 0.02-0.04 Hz, even though these sites are all at different areas of California.*

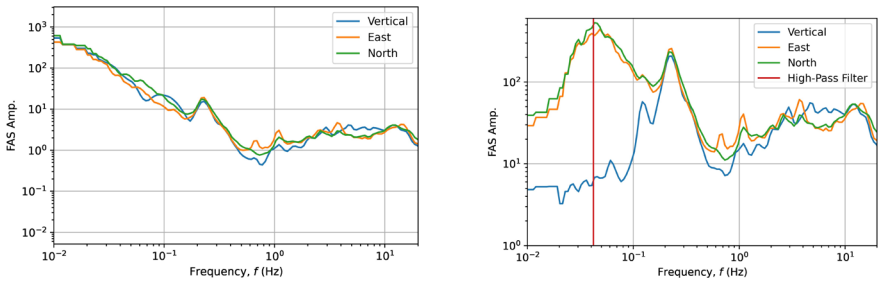


*Figure 7. (a) left: Fourier Amplitude Spectra (FAS) for site 2.250.2 in Benicia-Martinez South downhole vertical array with no high-pass corner filter applied. (b) right: FAS for site 2.250.2 in Benicia-Martinez South downhole vertical array with high-pass corner filter frequency of 0.042 Hz applied (shown by the blue vertical line). Note the strong drop off at low frequencies for the filtered vertical-component signal.*

## 4. Low Frequency Investigations

In this section, we investigate whether the low-frequency issues encountered with temporary instruments are also observed in a permanently-installed seismometer (Section 4.1). In addition, we investigate sensitivities to depth placements or sensors during temporary deployment (Section 4.2).

### 4.1. Co-Located Temporary and Permanent Instruments at Cabazon

A site in Cabazon, California was investigated. The permanent station is operated by the Southern California Seismic Network (SCSN) and has the station code CZN. The location is approximately 220 m south of the Union Pacific Railroad tracks. The permanent sensor is a Kinemetrics Mini Broadband Seismometer (MBB-2) with a flat response between 0.0083 Hz. and 160 Hz. Because the permanent sensor has been in place for a long period of time, the “settling” problems commonly encountered with temporary sensors are not expected to be present, so we wished to see if this would affect low-frequency mHVSR ordinates. During the temporary

deployment, two sensors were installed with partial burial (top of sensor is approximately at ground line) and burial with 46 cm (18 inches) of soil cover. We had been advised by Nanometrics that sensor burial could improve coupling and reduce the sensors' response to low-frequency noise and local slab-tilt. The sensors recorded data for about 3 hours. Data were also captured from the permanent seismometer near the sensor while the temporary data were recorded. Figures 8(a) and 8(b) show the time series for the data captured by the permanent seismometer and temporary seismometer during the daytime deployment. In both cases, the horizontal recordings lack drift, whereas the vertical components drift with the largest amount, somewhat surprisingly, from the permanent instrument. In addition, data at midnight were collected from the permanent sensor when anthropogenic noise levels are lower.

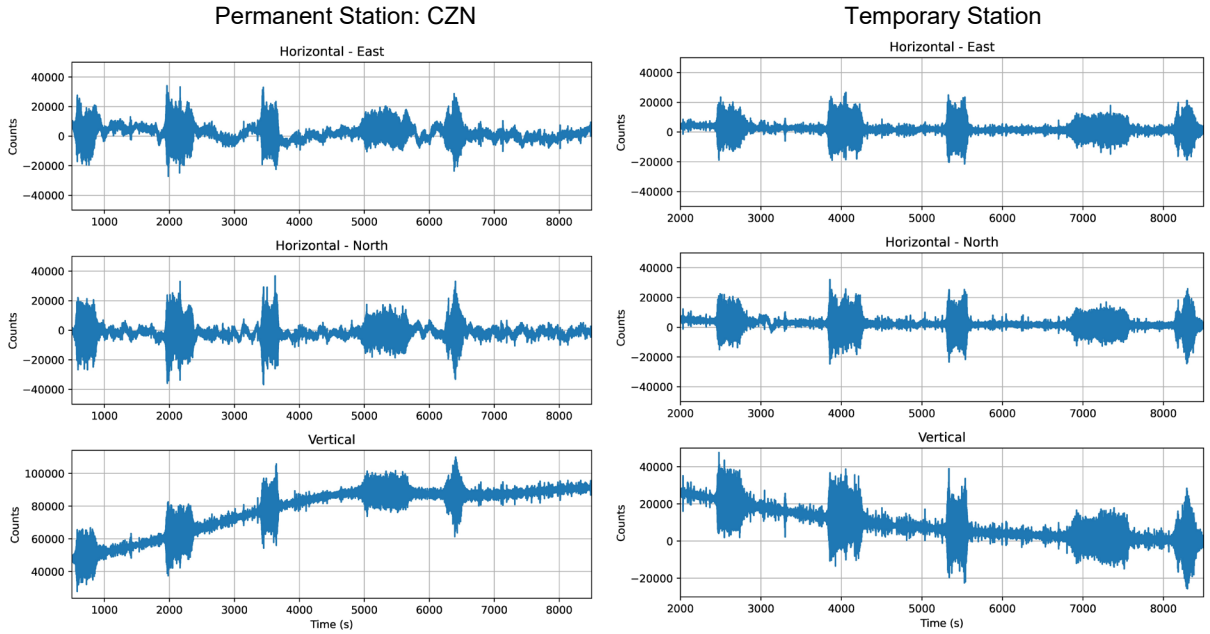


*Figure 8. (a) left: Raw time series for all three components of permanent station: CZN in Cabazon, showing the drift that is occurring in the vertical component for the recording that was done during the time that the temporary deployment was done. (b) right: Raw time series for all three components of the temporary 46 cm deployment at Cabazon, showing the drift that is occurring in the vertical component for the recording that was done during the time that the temporary deployment was done.*

These data were then processed using procedures described in Wang et al. (2022, 2023) and in the previous section, and mHVSR and power spectral density (PSD) curves were generated. PSD were computed using Obspy which is a library in Python that uses a routine by McNamara (2004). The reason for computing PSD curves was to facilitate comparisons of the ambient noise recorded at the Cabazon site to published noise models (Peterson 1993), which are expressed as PSD ordinates. Figure 9 compares the permanent and temporary PSD curves, which are seen to be very similar for the horizontal components. The vertical components have differences in which the data from the permanent seismometer in the daytime and at midnight have larger amplitudes than the recordings from the temporary deployment. This is likely caused by larger drift experienced in the permanent seismometer. Drift is not always encountered from permanent stations. At other sites (e.g., Network: CI (Southern California Seismic Network), Stations: SMF2(Santa Monica Airport), DRE(Desert Research Center, El Centro), LGB (Laguna Bell), we have found permanent stations to produce stationary vertical signals, which in turn produces relatively low-amplitude low-frequency mHVSR ordinates.

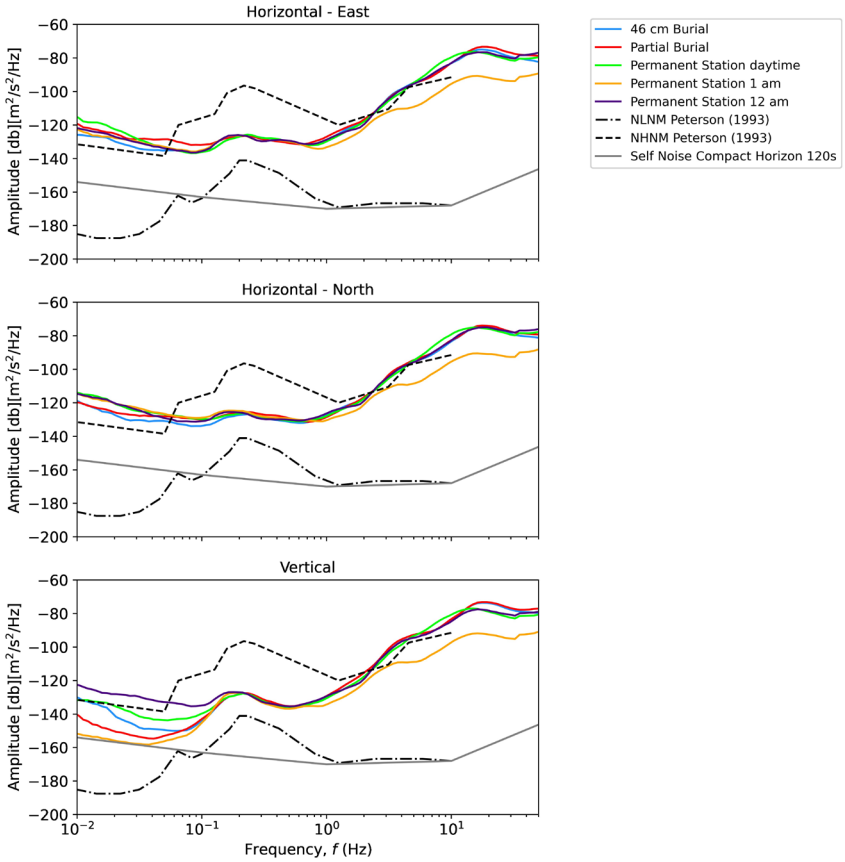


*Figure 9. Power Spectral Density (PSD) curves for station: CZN located in Cabazon, CA, showing the differences in instalment of temporary seismometer and the time difference of permanent seismometer data. The data are compared with the New Low Noise Model (NLNM) and New High Noise Model (NHNM) by Peterson (1993), to see the differences in noise levels between the temporary and permanent seismometers.*

Also shown in Figure 9 is the Peterson (1993) theoretical new low and high noise models (NLNM and NHNM; hereafter), which can be compared to the site data. The published self-noise of the temporary BB seismometer is also shown. In all components the noise levels are much higher than the NHNM of Peterson for frequencies below 0.06-0.07 Hz. Moreover, at frequencies above 2 Hz, the measured microtremor levels in all components are also higher than the NHNM levels. However, at frequencies between 0.07 and 2 Hz the noise levels are bound between the noise models. Based on the study from Wilson et. al. (2002), we might expect different noise sources at frequencies below 0.1 Hz relative to those at higher frequencies. Figure 9 shows elevated amplitudes below 0.1 Hz, which may reflect thermal or atmospheric variations at the site as asserted by Wilson et. al. (2002). At frequencies above 2 Hz the relatively high noise levels that exceed the models may be due to trains or an electrical substation nearby. However, in between these frequencies we get the most reliable data, and it is also where we are seeing resonant peaks in mHVSR.

Figure 10 compares the mHVSR curves produced from the different sensors and different times. When comparing the permanent station with the temporary deployment, the mHVSR curves are very similar for the case of the partial burial and the permanent. However, for the 46 cm burial the mHVSR mean curves have reduced amplitude, which had been suggested to be the effect of burial by Nanometrics. This is likely due to the fact that the sensor stabilized, and the drift experienced in the sensor dissipated, which can be seen in Figure 8(b). Comparisons of results from the permanent sensor for daytime and midnight reveal no significant differences. For frequencies greater than 0.1 Hz the curves are very similar, which likely means that the peaks at 0.5-1.0 Hz are likely true resonant peaks.

Figure 11 compares mHVSR for two types of time-windows: (1) windows with generally low and nearly uniform amplitudes (similar to Figures 4 and 6 (blue lines) and (2) windows with large amplitudes, most likely caused by trains). Interestingly, mHVSR low frequency ordinates for the large noise cases are significantly reduced

from the low-noise case, whereas at high frequencies there are no appreciable differences. This may be caused by the proximate noise source similarly affecting the vertical and horizontal components.

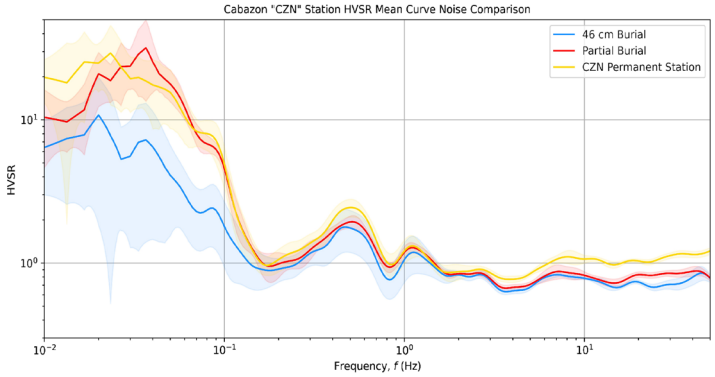


*Figure 10. mHVSR spectra for station CZN in Cabazon, CA, showing the differences at lower frequencies for permanent and temporary sensor deployments.*

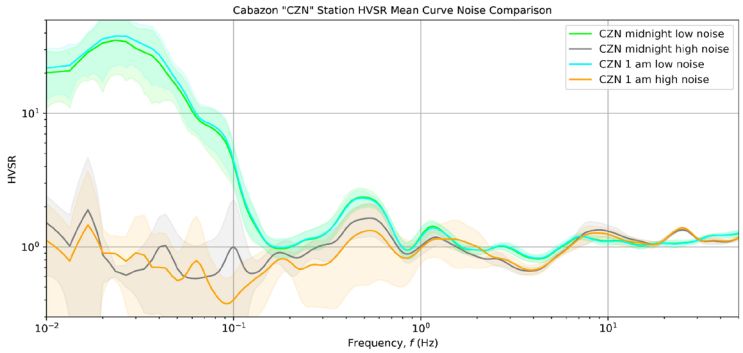


*Figure 11. mHVSR spectra for station: CZN located in Cabazon, CA, showing the differences between results for permanent sensors for time intervals with low and high noise.*

### 4.2. Sensor Deployments at Alternate Depths at Santa Monica Site

To investigate the effects of different sensor burial depths, we deployed multiple sensors at different depths at a shallow soil site outside of the Los Angeles Basin in Santa Monica, CA. This site does not have a permanently installed ground motion instrument.

mHVSR surveys were performed at four depths, resting at the surface, partially buried, buried 15 cm (distance from top of sensor to ground surface = 15 cm), and buried 30 cm. The sensors recorded data for three hours. The data were processed using similar procedures to those described above.

Figure 12 shows the resulting mHVSR for the different burial depths. In all cases, ordinates increase appreciably at low frequencies, as observed at the other sites discussed previously. The low-frequency ordinates generally decrease as burial depth increases, although curiously the surface sensor is counter to this trend. This decrease in amplitude from the surface sensor is likely due to an increased amount of noise in the vertical component producing smaller amplitude mHVSR ordinates as discussed in the previous section. The source of the noise may be from coupling issues or local slab-tilt, which seem to greatly affect surface mounted mHVSR surveys, causing high amplitude vertical noise. Figure 12 shows this high amplitude low-frequency peak occurring again at about 0.04 Hz.

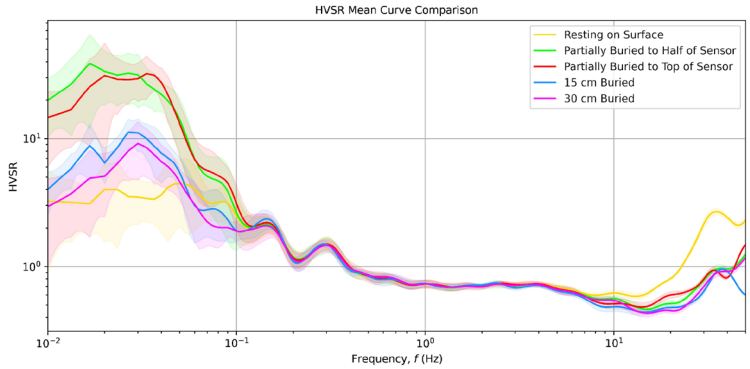


*Figure 12. mHVSR spectra for a site in Santa Monica, CA, showing the differences of how at lower frequencies there much variation with the curves is due to the different instalments.*

### 4.3. Findings from Investigations

These investigations show the following principal results:

1. Burying sensors at different depths, as suggested by Nanometrics, affects low-frequency mHVSR ordinates, but does not solve the problem of unrealistically high amplitude ordinates at low frequencies.
2. Both permanent and temporary sensors can demonstrate high-amplitude ordinates at low frequencies. Where this occurs, it may be an attribute of localized slab-tilt distorting our results at low frequencies (< ~0.1-0.2 Hz). However, in some cases drift is absent in permanent stations, and the conditions leading to drift or lack thereof are poorly understood. The implications for mHVSR applications are important, because when drift is present it appears that we cannot detect site resonant peaks at frequencies below about 0.1 to 0.2 Hz.

## 5. Conclusions

We have shown that low-frequency mHVSR ordinates from temporary sensor deployments appear to not have the potential to characterize geologic structure at great depths. The cause of this is uncertain, but based on prior literature, it may be related to localized slab-tilt which in turn is greatly affected by thermal and barometric effects (Wilson et. al. 2002). Ongoing research aims to identify the cause of such effects at low frequencies. We plan on performing more mHVSR tests from temporary deployments, and analysing data from permanent sensors, to more robustly establish conditions that do and do not lead to vertical-component drift. Moreover, we plan to further examine the influence of processing procedures on the large-amplitude peak formed from low-frequency noise, including filtering, windowing, and tapers.

## 6. Acknowledgements

The research presented here was supported by a research gift from Pacific Gas and Electric Company. This support is gratefully acknowledged.

## 7. References

Afshari, K, JP Stewart, JH Steidl (2019). California ground motion vertical array database, *Earthquake Spectra*, **35**, 2003-2015.

Bonilla, L. F., J. H. Steidl, J.-C. Gariel, and R. J. Archuleta (2002). Borehole response studies at the Garner Valley downhole array, Southern California, Bull. Seismol. Soc. Am. 92, 3165–3179.

Butterworth, S., “On the Theory of Filter Amplifiers,” Experimental Wireless and the Wireless Engineer, Vol. 7, 1930, pp. 536-541.

Cadet, H., P.-Y. Bard, A.-M. Duval, and E. Bertrand (2012). Site effect assessment using KiK-net data: Part 2—Site amplification prediction equation based on f0 and Vsz, Bull. Earthq. Eng. 10, 451–489.

de la Torre, C., Bradley, B., Stewart, J., McGann, R. (2022). “Can modeling soil heterogeneity in 2D site response analyses improve predictions at vertical array sites?” Earthquake Spectra, Vol. 38, No. 4.

Ghofrani, H., G. M. Atkinson, and K. Goda (2013). Implications of the 2011 M9.0 Tohoku Japan earthquake for the treatment of site effects in large earthquakes, Bull. Earthq. Eng. 11, 171–203.

Given, H. K., and F. Fels (1993). Site characteristics and ambient ground noise at IRIS IDA stations AAK (Ala-Archa, Kyrgyzstan) and LY (Talaya, Russia), *Bull. Seism. Soc. Am.* 83, 945–953.

Kawase, H., F. J. Sánchez-Sesma, and S. Matsushima (2011). The optimal use of horizontal-to-vertical spectral ratios of earthquake motions for velocity inversions based on diffuse-field theory for plane waves, Bull. Seismol. Soc. Am. 101, 2001–2014.

Lachet, D., C. Hatzfeld, P.-Y. Bard, N. Theodulis, C. Papaioannou, and A. Savvaidis (1996). Site effects and microzonation in the city of Thessaloniki (Greece): Comparison of different approaches, Bull. Seismol. Soc. Am. 86, 1692–1703.

Lermo, J., and F. J. Chávez-García (1993). Site effect evaluation using spectral ratios with only one station, Bull. Seismol. Soc. Am. 83, 1574–1594.

McNamara, D. E. and Buland, R. P. (2004), Ambient Noise Levels in the Continental United States, *Bulletin of the Seismological Society of America*, 94 (4), 1517-1527. http://www.bssaonline.org/content/94/4/1517.abstract

Nakamura, Y. (1989). A method for dynamic characteristics estimation of subsurface using microtremors on the ground surface, Quarterly Report of Railway Technical Research Institute (RTRI), 30, 25-33.

Ornelas, F., C. de la Torre, C. Nweke, T. Buckreis, P. Wang, B. Bradley, S. Brandenberg, J. Stewart. (Year appears in Published) "Microtremor Horizontal-to-Vertical Spectral Ratio (mHVSR) Data Collection at California Downhole Vertical Array Sites, 2022", in *Microtremor Horizontal-to-Vertical Spectral Ratio (mHVSR) Site Characterization of California Vertical Arrays*. DesignSafe-CI. https://doi.org/10.17603/ds2-by4m-ed67

Site EffectS assessment using AMbient Excitations (SESAME) (2004). Guidelines for the implementation of the H/V spectral ratio technique on ambient vibrations—Measurements, processing and interpretation, European Commission Project No. EVG1-CT- 2000-00026, 62, available at http://sesame.geopsy.org/Papers/HV_User_Guidelines.pdf (last accessed September 2012).

Theodulidis, N., R. J. Archuleta, P.-Y. Bard, and M. Bouchon (1996). Horizontal to vertical spectral ratio and geological conditions: The case of Garner Valley downhole array in southern California, Bull. Seismol. Soc. Am. 86, 306–319.

Tukey, J.W. (1967). "An introduction to the calculations of numerical spectrum analysis". *Spectral Analysis of Time Series*: 25–46.

Wang, P. (2021). wltcwpf/hvsrProc: First release (v1.0.0), Zenodo, doi:10.5281/zenodo.4724141.

Wang, P., P. Zimmaro, and J. P. Stewart (2021). Horizontal-to-vertical spectral ratio database access and analysis, DesignSafe-CI. PRJ-3085 doi: 10.17603/ds2-nn2e-wm79.

Wang, P., P. Zimmaro, T. E. Buckreis, T. Gospe, S. J. Brandenberg, S. K. Ahdi, A. Yong, and J. P. Stewart (2022). Relational Database for Horizontal-to-Vertical Spectral Ratios, Seismol. Res. Lett. 93, 1075–1088, doi: 10.1785/0220210128.

Wang, P, P Zimmaro, SK Ahdi, A Yong, JP Stewart (2023). Identification protocols for horizontal-to-vertical spectral ratio peaks, *Bull. Seismol. Soc. Am.*, **113**(2), 782-803.

Wathelet, M., J.-L. Chatelain, C. Cornou, G. Di Giulio, B. Guillier, M. Ohrnberger, and A. Savvaidis (2020). Geopsy: A user-friendly open-source tool set for ambient vibration processing, Seismol. Res. Lett. 91, 1878–1889, doi: 10.1785/0220190360.

Wilson, D., J. Leon, R. Aster, J. Ni, J. Schlue, S. Grand, S. Semken, S. Baldridge, and W. Gao (2002). Broadband seismic background noise at temporary seismic station observed on a regional scale in the southwestern United States, *Bulletin of the Seismological Society* of America, 92 (8), 3,335-3,342.